Weierstraß-Institut

für Angewandte Analysis und Stochastik

Leibniz-Institut im Forschungsverbund Berlin e. V.

Preprint ISSN 2198-5855

Comparison and numerical treatment of generalised Nernst–Planck Models

Jürgen Fuhrmann

Weierstrass Institute
Mohrenstr. 39
10117 Berlin
Germany
email: juergen.fuhrmann@wias-berlin.de

submitted: April 8, 2014

No. 1940
Berlin 2014

2010 *Mathematics Subject Classification.* 65N08,78A57.

2010 *Physics and Astronomy Classification Scheme.* 82.45.Gj.

Key words and phrases. Electrolytes, Nernst-Planck equations, Bikerman-Freise Model, Finite Volume Methods.

This research was carried out in the framework of the project “Macroscopic Modeling of Transport and Reaction Processes in Magnesium-Air-Batteries” (Grant 03EK3027D) under the research initiative “Energy storage” of the German Federal government.

Edited by
Weierstraß-Institut für Angewandte Analysis und Stochastik (WIAS)
Leibniz-Institut im Forschungsverbund Berlin e. V.
Mohrenstraße 39
10117 Berlin
Germany

Fax: +49 30 20372-303
E-Mail: preprint@wias-berlin.de
World Wide Web: http://www.wias-berlin.de/

ABSTRACT. In its most widespread, classical formulation, the Nernst–Planck–Poisson system for ion transport in electrolytes fails to take into account finite ion sizes. As a consequence, it predicts unphysically high ion concentrations near electrode surfaces. Historical and recent approaches to an approriate modification of the model are able to fix this problem. Several appropriate formulations are compared in this paper. The resulting equations are reformulated using absolute activities as basic variables describing the species amounts. This reformulation allows to introduce a straightforward generalisation of the Scharfetter-Gummel finite volume discretization scheme for drift-diffusion equations. It is shown that it is thermodynamically consistent in the sense that the solution of the corresponding discretized generalized Poisson–Boltzmann system describing the thermodynamical equilibrium is a stationary state of the discretized time-dependent generalized Nernst–Planck system. Numerical examples demonstrate the improved physical correctness of the generalised models and the feasibility of the numerical approach.

1. INTRODUCTION

The motion of an incompressible mixture of $N-1$ ionic species and an electroneutral solvent component N in the self-consistent electrical field can be described by system consisting of $N-1$ Nernst–Planck equations for the motion (relative to the barycentric velocity) of the ions, the Poisson equation for the electrostatic field, and the Navier–Stokes equations for the barycentric velocity of the mixture with a body force depending on the space charge and the electric field. Mostly, throughout the paper, the fluid motion will be regarded in mechanical equilibrium. Electrochemistry and semiconductor devices are two main applications of systems of this type.

The classical drift diffusion approach assumes the species concentration gradient (with a constant diffusion coefficient), the advection by barycentric velocity and the advection by the gradient of the electrostatic potential as driving forces for the motion of charged species the self-consistent electric field [NTA12]. It is well known for a long time, that for electrolytes, this approach fails to reflect the fact that ion sizes are finite. After a first improvement in [Ste24], starting with [Bik42], various volume exclusion models have been proposed to fix this problem with varying generality and success [Bik42, Fre52, Spa58, CS69, MCSJ71, KV81, MR02, Tre08], see also the reviews of [BS07, BKSA09].

Nonequilibrium thermodynamics [dGM62] suggests that the chemical potentials of the species have to be regarded as driving forces, allowing to describe finite ion size effects in the constitutive relationship between chemical potential and concentration. The authors of [DGM13] recently confirmed that in order to derive a thermodynamically consistent model is necessary to include the dependency on the pressure into this relationship [Fre52].

In section 2, the Nernst–Planck–Poisson–Navier–Stokes system for an ideal incompressible mixture is introduced in a formulation equivalent to that provided in [DGM13]. Then, constitutive relationships between chemical potential, pressure and concentration are introduced for four cases: the classical Nernst–Planck equations leading to the Gouy-Chapman double layer model, the excluded volume models after

Bikerman and Freise [Bik42, Fre52], the ideal incompressible mixture [DGM13], and — as it is closely related — Fermi–Dirac statistics for semiconductor problems. It is shown that in thermodynamical equilibrium and for the case of equal molar masses, the ideal incompressible mixture model [DGM13] is equivalent to a multispecies generalization of the Bikerman–Freise model.
In section 3, with the intention to provide a reliable numerical implementation, the models under investigation are reformulated in absolute activities as basic variables. This reformulation results in a rather simple structure of the resulting system of equations. In particular, cross-coupling of species gradients and degenerating diffusion coefficients are avoided. This formulation as well allows for an easy expression of the equations for thermodynamical equilibrium.
In section 4, based on the Scharfetter-Gummel upwind method [SG69], a finite volume based multi-dimensional numerical approach to the approximate solution of the coupled systems is proposed. It is shown that the discrete solution of the corresponding equilibrium generalized Poisson–Boltzmann problem is a stationary solution of the discretized generalized Nernst–Planck system. Numerical examples demonstrate the features of the diffrent models dicussed, and the feasibility of the discretization approach.
All notations are listed in appendix A. Appendix B provides the link of the model described in section 2 to the formulation used in [DGM13]. In order to support the proposal to formulate the equations in activities as primary variables, appendix C discusses the consequences of using concentrations as basic unknowns. Appendix D is devoted to the mathematical proof of the existence and uniqueness of the inverse activity coefficients.

2. The Nernst–Planck–Poisson–Navier–Stokes–System

In this section, the Nernst–Planck–Poisson–Navier–Stokes system for an isothermal, incompressible ideal mixture without ion size and solvation effects, representing a solution of $N-1$ dissolved species characterised by molar densities (in the sequel colloquially referred to as "concentrations") c_α and molar chemical potentials μ_α in an electroneutral solvent component N is introduced. Different variants for constitutive laws for the chemical potentials are discussed. All notations are found in appendix A. For a given distribution of the barycentric velocity $\mathbf{v}$, the evolution of the molar concentrations c_α of charged species is described by the Nernst–Planck–Poisson system [dGM62, DGM13], see also appendix B:

$$-\nabla \varepsilon_0 \varepsilon_r \nabla \phi = q \tag{2.1a}$$

$$\partial_t c_\alpha + \nabla \cdot (c_\alpha \mathbf{v} + \mathbf{N}_\alpha) = 0 \qquad \alpha = 1 \dots N-1 \tag{2.1b}$$

$$\mathbf{N}_\alpha = -\frac{D_\alpha}{RT} c_\alpha \left(\nabla \mu_\alpha - \frac{M_\alpha}{M_N} \nabla \mu_N + z_\alpha F \nabla \phi \right) \qquad \alpha = 1 \dots N-1. \tag{2.1c}$$

In the effective chemical potentials

$$\tilde{\mu}_\alpha = \mu_\alpha - \frac{M_\alpha}{M_N} \mu_N \quad (\alpha = 1 \dots N-1) \tag{2.2}$$

the Nernst–Planck equation (2.1c) rewrites as

$$\mathbf{N}_\alpha = -\frac{D_\alpha}{RT} c_\alpha \left(\nabla \tilde{\mu}_\alpha + z_\alpha F \nabla \phi \right), \qquad (\alpha = 1 \dots N-1). \tag{2.3}$$

As in [dGM62], the N diffusion fluxes $\mathbf{J}_\alpha = M_\alpha \mathbf{N}_\alpha$ sum up to zero. The solvent concentration

$$c_N = \bar{c} - \sum_{\alpha=1}^{N-1} c_\alpha \tag{2.4}$$

is the difference between the constant (due to incompressibility, see appendix B.2) concentration $\bar{c}$ of the mixture and the sum of the concentrations of the dissolved species.
The evolution of the velocity field is described by the incompressible Navier–Stokes equations for the barycentric velocity $\mathbf{v}$ and the pressure p under a body force exerted by the motion of ions:

$$\partial_t(\rho\mathbf{v}) + \nabla\cdot(\rho\mathbf{v}\otimes\mathbf{v}) - \eta\Delta\mathbf{v} + \nabla p = -q\nabla\phi \tag{2.5a}$$

$$\partial_t\rho + \nabla\cdot(\rho\mathbf{v}) = 0 \tag{2.5b}$$

$$\rho = M_N\bar{c} + \sum_{\alpha=1}^{N-1}(M_\alpha - M_N)c_\alpha \tag{2.5c}$$

One should note that the density ρ is dependent on the local composition of the mixture. From [dGM62], replacing specific quantities by molar ones, note the Gibbs-Duhem relation

$$\sum_{\alpha=1}^{N} c_\alpha \nabla\mu_\alpha = \nabla p. \tag{2.6}$$

In the case of mechanical equilibrium characterised by $\partial_t\mathbf{v} = 0, \nabla\mathbf{v} = 0$, the Navier–Stokes equations (2.5) reduce to the force balance [dGM62]

$$\nabla p = -q\nabla\phi. \tag{2.7}$$

Taking the divergence on both sides of (2.7) gives

$$-\Delta p = \nabla\cdot q\nabla\phi. \tag{2.8}$$

As it can be assumed that far from an electrode, the pressure p can be set equal to a fixed reference pressure p°, (2.8) is a variant of the force balance (2.7) which leads to a second order partial differential equation for the pressure p which can be treated by standard analytical and numerical tools.
In order to close system (2.1), it is necessary to introduce constitutive relationships between the chemical potentials $\mu_1 \dots \mu_N$ and the other quantities describing the system.

2.1. **Chemical potential for classical Nernst–Planck theory.** In this theory, it is assumed that the motion of the solvent is not influenced by the motion of the dissolved species, and the chemical potential can be set to [AdP06]. The chemical potential of the solvent is set to $\mu_N = 0$, leading to $\tilde{\mu}_\alpha = \mu_\alpha$ for $\alpha = 1 \dots N-1$. It is then assumed that the the chemical potential follows the ansatz for an ideal gas:

$$\tilde{\mu}_\alpha^{\mathrm{GC}} = \mu_\alpha = \mu_\alpha^\circ + RT\ln\frac{c_\alpha}{\bar{c}} \quad (\alpha = 1\dots N-1). \tag{2.9}$$

It corresponds to the Gouy–Chapman double layer model [BF80] and is therefore labeled as “GC”. This ansatz regards ions as point charges and misses the fact that the finite size of real ions limits the maximum possible species concentrations c_α. In [DGM13] it has been criticised for not being consistent with the approach of non-equilibrium thermodynamics.

2.2. **Chemical potential for excluded volume models.** The deficiencies of the model (2.9) have been known since a long time, and the introduction of an excluded volume constraint is the subject of a significant number of papers, e.g. [Bik42, Fre52, Spa58, CS69, MCSJ71, KV81, MR02, Tre08]. See also the reviews of [BS07, BKSA09].
The summary volume fraction of the dissolved species amounts to

$$\Phi = \sum_{\alpha=1}^{N-1} v_\alpha c_\alpha, \tag{2.10}$$

where v_α is the partial molar volume which can be defined as the volume necessary to accommodate 1 mol of species α together with the hydration shells [BS07]. Given the value Φ, the standard way to incorporate the volume constraint amounts to set $\mu_N = 0$ and

$$\mu_\alpha = \tilde{\mu}_\alpha = \mu_\alpha^\circ + RT \ln \frac{c_\alpha}{\bar{c}} - RT \ln(1-\Phi). \qquad (\alpha = 1 \ldots N-1) \tag{2.11}$$

Alternative approaches based on hard sphere models assume rational expressions $R_\alpha(\Phi)$ in Φ instead of the second logarithm in (2.11) [CS69, MCSJ71, BS07]. Besides of the attempt of [Tre08] it seems to be an open question if these models are consistent to the approach of non-equilibrium thermodynamics.
The partial molar volume v_α can be estimated from the excluded volume v_α^{excl} of a single ion in a sphere packing $v_\alpha = N_A v_\alpha^{excl}$. The excluded volume can be estimated from the radius of the solvated ion r_α. E.g. in [PDK+96], it is assumed that it is eight times the volume of the sphere with radius r_α yielding $v_\alpha = 8 N_A \frac{4}{3}\pi r_\alpha^3$. An alternative estimate of this value which attempts to be consistent with the axioms of non-equilibrium thermodynamics can be found in [Tre08].
The Bikerman–Freise model [Bik42, Fre52] assumes that all molecules are placed on one given lattice with lattice constant a and that $v_\alpha = v = a^3$. A particular choice is $v = \frac{1}{\bar{c}}$ which is consistent to (2.4) and results in

$$1 - \Phi = \frac{c_N}{\bar{c}} \tag{2.12}$$

Originally derived for two species, its generalisation for the multi-species case is straightforward:

$$\begin{aligned} \tilde{\mu}_\alpha^{\mathrm{BF}} &= \mu_\alpha^\circ + RT \ln \frac{c_\alpha}{\bar{c}} - RT \ln \frac{c_N}{\bar{c}} \\ &= \mu_\alpha^\circ + RT \ln \frac{c_\alpha}{\bar{c}} - RT \ln \left(1 - \sum_{\alpha=1}^{N-1} \frac{c_\alpha}{\bar{c}}\right). \end{aligned} \tag{2.13}$$

2.3. **Chemical potential of an incompressible ideal mixture.** The authors of [DGM13] derive the chemical potential assuming a thermodynamically consistent free energy for a compressible mixture. The resulting chemical potential depends on the pressure. This pressure dependency remains in the incompressible limit (see appendix B):

$$\mu_\alpha = \mu_\alpha^\circ + \frac{1}{\bar{c}}(p - p^\circ) + RT \ln \frac{c_\alpha}{\bar{c}}. \qquad (\alpha = 1 \ldots N) \tag{2.14}$$

This choice is consistent the the Gibbs-Duhem relation (2.6):

$$\sum_{\alpha=1}^{N} c_\alpha \nabla \mu_\alpha = \sum_{\alpha=1}^{N} \frac{c_\alpha}{\bar{c}} \nabla p + \sum_{\alpha=1}^{N} RT c_\alpha \nabla \ln \frac{c_\alpha}{\bar{c}} \tag{2.15}$$

$$= \nabla p \frac{\sum_{\alpha=1}^{N} c_\alpha}{\bar{c}} + RT\bar{c}\nabla(\sum_{\alpha=1}^{N} c_\alpha) = \nabla p \tag{2.16}$$

The resulting effective chemical potential is

$$\tilde{\mu}_\alpha^{\mathrm{DGM}} = \tilde{\mu}_\alpha^\circ + RT \ln \frac{c_\alpha}{\bar{c}} + \left(1 - \frac{M_\alpha}{M_N}\right) \frac{(p - p^\circ)}{\bar{c}} - \frac{M_\alpha}{M_N} RT \ln \frac{c_N}{\bar{c}}, \quad (\alpha = 1 \ldots N-1). \tag{2.17}$$

The following statement regards some limiting cases of potential interest.

Lemma 2.1. *The following equivalences hold (possibly up to a difference in the constant reference chemical potential):*

(i) For equal molar weights $M_\alpha = M_N$ ($\alpha = 1 \ldots N-1$), the chemical potential of an ideal incompressible mixture is equivalent to that of the excluded volume model with molar volume $v = \frac{1}{\bar{c}}$:

$$\tilde{\mu}_\alpha^{\mathrm{DGM}} = \tilde{\mu}_\alpha^{\mathrm{BF}} = \tilde{\mu}_\alpha^\circ + RT \ln \frac{c_\alpha}{\bar{c}} - RT \ln \left(1 - \sum_{\alpha=1}^{N-1} \frac{c_\alpha}{\bar{c}}\right) \tag{2.18}$$

(ii) In the case of light ions and heavy solvent $M_\alpha << M_N$ ($\alpha = 1 \ldots N-1$), the chemical potential of an ideal incompressible mixture reduces to the pressure correction model

$$\tilde{\mu}_\alpha^{\mathrm{PC}} = \mu_\alpha^\circ + RT \ln \frac{c_\alpha}{\bar{c}} + \frac{1}{\bar{c}}(p - p^\circ). \tag{2.19}$$

(iii) In thermodynamical equilibrium,

$$\tilde{\mu}_\alpha^{\mathrm{DGM}} = \tilde{\mu}_\alpha^{\mathrm{BF}} = \tilde{\mu}_\alpha^{\mathrm{PC}}. \tag{2.20}$$

Proof. Obviously, statements (i) and (ii) immediately follow from (2.17). It remains to regard (iii).
The thermodynamical equilibrium is characterised by $\mathbf{N}_\alpha = 0$ for $\alpha = 1 \ldots N$. By summing up all fluxes, one obtains

$$\begin{aligned}
0 = \sum_{\alpha=1}^{N-1} \frac{RT}{D_\alpha} \mathbf{N}_\alpha &= \sum_{\alpha=1}^{N-1} c_\alpha \left(\nabla \mu_\alpha - \frac{M_\alpha}{M_N} \nabla \mu_N + F z_\alpha \nabla \phi \right) \\
&= \sum_{\alpha=1}^{N-1} \left(c_\alpha \nabla \mu_\alpha - c_\alpha \frac{M_\alpha}{M_N} \nabla \mu_N \right) + q \nabla \phi \\
&= \sum_{\alpha=1}^{N} c_\alpha \nabla \mu_\alpha - c_N \nabla \mu_N - \frac{1}{M_N} \nabla \mu_N \sum_{\alpha=1}^{N-1} M_\alpha c_\alpha + q \nabla \phi \\
&\overset{(2.6)}{=} \nabla p + q \nabla \phi + \frac{1}{M_N} \nabla \mu_N \sum_{\alpha=1}^{N} M_\alpha c_\alpha \\
&\overset{(2.7)}{=} \frac{\rho}{M_N} \nabla \mu_N.
\end{aligned}$$

As a consequence, μ_N is constant, and

$$\frac{1}{\bar{c}}(p - p^\circ) = \mu_N - \mu_N^\circ - RT \ln \frac{c_N}{\bar{c}},$$

stating that in thermodynamical equilibrium, the pressure contribution to the chemical potential is equivalent to the excluded volume contribution. □

2.4. **Chemical potential for general carrier statistics.** General statistics functions linking concentration and chemical potential are discussed in particular in semiconductor device theory:

$$c_\alpha = c\mathscr{G}\left(\frac{\mu_\alpha - \mu_\alpha^\circ}{RT}\right). \tag{2.21}$$

Mostly, the functions $\mathscr{G}$ are Fermi–Dirac integrals of different orders

$$\mathscr{G}(\eta) = \mathscr{F}_j(\eta) = \frac{1}{\Gamma(j+1)}\int_0^\infty \frac{\xi^j}{1+\exp(\xi-\eta)}d\xi \tag{2.22}$$

or their approximations. Of particular interest for electrolytes is the Fermi–Dirac integral of order -1

$$\mathscr{F}_{-1}(\eta) = \frac{1}{1+\exp(-x)}. \tag{2.23}$$

The corresponding chemical potential model assumes $\mu_N = 0$ and [KV81, LFJ11]

$$\tilde{\mu}_\alpha^{\mathrm{FD}} = \mu_\alpha^\circ + RT\ln\frac{c_\alpha}{\bar{c}} - RT\ln\left(1-\frac{c_\alpha}{\bar{c}}\right). \tag{2.24}$$

which is a simplification of expression (2.13) by ignoring the interaction of different species. It however keeps the constraint of the ion size.

3. Reformulation in absolute effective activities

From the thermodynamical point of view, the chemical potentials are naturally continuous amounts, and their gradients are natural driving forces for species transport. However, in numerical calculations, one would encounter difficulties with approximating small concentrations, due to the fact that the notation of zero concentration does not exist as the chemical potentials tend to $-\infty$ as concentration tends to 0. A number of complications in the expressions arising from the transformation to concentrations is exhibited in appendix C. In addition to the fact that concentrations in general are not continuous at material interfaces, these complications offset the advantages of this formulation. This section discusses the reformulation of the flux terms using absolute activities as basic variables.

The *absolute activity* λ_α of a species is defined as [IUP14] $\lambda_\alpha = \exp\frac{\mu_\alpha}{RT}$, while the *relative activity* a_α is defined as $a_\alpha = \exp\frac{\mu_\alpha - \mu_\alpha^\circ}{RT}$. As at interfaces between different media, reference chemical potentials may jump, whereas chemical potentials are continuous, an activity based reformulation should start from absolute activities, as these inherit continuity from the chemical potential. Based on the effective chemical potentials, one introduces the *absolute effective activity*. For brevity, in this paper it will be referred to as "activity" and it will be denoted by a_α:

$$a_\alpha = \exp\frac{\tilde{\mu}_\alpha}{RT}. \tag{3.1}$$

Using the (absolute effective) *activity coefficient* γ_α defined by $a_\alpha = \gamma_\alpha\frac{c_\alpha}{\bar{c}}$, one can express $c_\alpha = \bar{c}\frac{a_\alpha}{\gamma_\alpha}$. Then $\beta_\alpha(a_1, a_2, \ldots, a_{N-1}, p) = \frac{1}{\gamma_\alpha}$ denotes the (absolute effective) *inverse activity coefficient* of species α. It allows to express

$$c_\alpha = \bar{c}\beta_\alpha a_\alpha. \tag{3.2}$$

All specific expressions characterising a particular constitutive relationship for the chemical potential are transformed to particular expressions for β_α. The Nernst–Planck flux rewrites as

$$\mathbf{N}_\alpha = -\frac{D_\alpha}{RT} c_\alpha \left(\nabla \tilde{\mu}_\alpha + z_\alpha F \nabla \phi\right) = -\frac{D_\alpha}{RT} \bar{c} \beta_\alpha a_\alpha \left(\frac{RT}{a_\alpha} \nabla a_\alpha + z_\alpha F \nabla \phi\right), \tag{3.3}$$

and the full Nernst–Planck–Poisson system (2.1) becomes

$$-\nabla \cdot \varepsilon_0 \varepsilon_r \nabla \phi = q \tag{3.4a}$$

$$\partial_t (\bar{c} \beta_\alpha a_\alpha) + \nabla \cdot \left(\bar{c} \beta_\alpha a_\alpha \mathbf{v} + \mathbf{N}_\alpha\right) = 0 \qquad \alpha = 1 \ldots N-1 \tag{3.4b}$$

$$\mathbf{N}_\alpha = -D_\alpha \bar{c} \beta_\alpha \left(\nabla a_\alpha + a_\alpha z_\alpha \frac{F}{RT} \nabla \phi\right) \quad \alpha = 1 \ldots N-1 \tag{3.4c}$$

$$q = \bar{c} F \sum_{\alpha=1}^{N-1} z_\alpha \beta_\alpha a_\alpha \tag{3.4d}$$

One observes that under the time derivative and the divergence operator, expressions in the activities occur which are formally equal to the rather well understood classical Nernst–Planck case, and which are multiplied by the inverse activity coefficients.

3.1. **Gouy–Chapman model.** In this case, the activity a_α is identical to the mole fraction $\frac{c_\alpha}{\bar{c}}$, and

$$\beta_\alpha^{\mathrm{GC}} = 1 \qquad (\alpha = 1 \ldots N-1). \tag{3.5}$$

3.2. **Bikerman–Freise model.** In this case, it is easy to see that the inverse activity coefficients have to be obtained from the solution of a linear system of equations

$$a_\alpha^\circ \beta_\alpha = 1 - \sum_{i=1}^{N-1} \beta_i a_i \qquad (\alpha = 1 \ldots N-1). \tag{3.6}$$

where $a_\alpha^\circ = \exp\left(\frac{\mu_\alpha^\circ}{RT}\right)$, is the reference activity.

Lemma 3.1. *Under the condition that $a_\alpha^\circ > 0, a_\alpha \geq 0$, system* (3.6) *has an unique bounded positive solution*

$$\beta_\alpha^{\mathrm{BF}} = \frac{1}{a_\alpha^\circ \left(1 + \sum_{i=1}^N \frac{a_i}{a_i^\circ}\right)} < \frac{1}{a_\alpha^\circ}, \qquad (\alpha = 1 \ldots N-1). \tag{3.7}$$

Proof. See appendix D. □

Comparing to the concentration based case (C.2), one observes that no gradient coupling is introduced. The flux is a type of nonlinear drift-diffusion flux of the activities, where the mobility coefficient for one species depends on the activities of the other species, but not on their gradients. Of particular interest is the fact that the inverse activity coefficient does not degenerate. As a_α tends to ∞, the concentration tends to one, provided all other activities are limited.

3.3. **Incompressible ideal mixture.** in the case of pure pressure correction (2.19) one has

$$\beta_\alpha^{\mathrm{PC}} = \frac{1}{a_\alpha^\circ} \exp\left(-\frac{p-p^\circ}{\bar{c}RT}\right) \qquad (\alpha = 1\ldots N-1). \tag{3.8}$$

In difference to a concentration based formulation, no pressure gradients occur in the resulting version of the Nernst–Planck equation, see (C.3).
In the general case (2.17), the inverse activity coefficients are the solution of a nonlinear system of equations:

$$\beta_\alpha = \frac{1}{a_\alpha^\circ} \exp\left(-\frac{p-p^\circ}{\bar{c}RT}\right)^{1-\frac{M_\alpha}{M_N}} \left(1 - \sum_{i=1}^{N-1} \beta_i a_i\right)^{\frac{M_\alpha}{M_N}} \qquad (\alpha = 1\ldots N-1). \tag{3.9}$$

Lemma 3.2. *Under the condition that $a_\alpha^\circ > 0, a_\alpha \geq 0$, system* (3.9) *has an unique bounded positive solution*

$$0 < \beta_\alpha^{\mathrm{DGM}} < \frac{1}{a_\alpha^\circ} \exp\left(-\frac{p-p^\circ}{cRT}\right)^{1-\frac{M_\alpha}{M_N}}. \tag{3.10}$$

Proof. See appendix D. □

3.4. **Fermi–Dirac model.** The inverse activity coefficient in the case of general statistics is $\beta_\alpha(a_\alpha) = \frac{\mathscr{G}\left(\ln \frac{a_\alpha}{a_\alpha^\circ}\right)}{a_\alpha}$, in particular, in the case $\mathscr{G} = \mathscr{F}_{-1}$, one obtains

$$\beta_\alpha^{\mathrm{FD}} = \frac{1}{a_\alpha^\circ + a_\alpha}. \tag{3.11}$$

One again recognises, that this can bee seen as a variant of the Bikerman–Freise model (3.7) which however ignores the interaction between different species. When comparing to the case of the diffusion enhancement (C.8), one observes, that no degeneration is introduced. As a_α tends to ∞, the concentration tends to one.

3.5. **Equilibrium case: Nonlinear Poisson System.** Using the the activity based flux expressions it is straightforward to derive expressions for the corresponding modified Poisson–Boltzmann equations describing thermodynamical equilibrium. At the same time, mechanical equilibrium is assumed. Assuming zero flux due to thermodynamical equilibrium, one arrives at

$$\nabla \tilde{\mu}_\alpha = -z_\alpha F \nabla \phi \qquad \alpha = 1\ldots N-1. \tag{3.12}$$

One possibility describe this situation is to introduce the constant quasi-Fermi (electrochemical) potential ψ_α and to set $\tilde{\mu}_\alpha = z_\alpha F(\psi_\alpha - \phi)$ leading to a coupled differential-algebraic system

$$-\nabla \varepsilon_0 \varepsilon_r \nabla \phi = Fc \sum_{\alpha=1}^{N-1} z_\alpha \beta_\alpha a_\alpha \tag{3.13}$$

$$a_\alpha = \exp\left(\frac{z_\alpha F}{RT}(\psi_\alpha - \phi)\right) \qquad (\alpha = 1\ldots N-1). \tag{3.14}$$

For the Gouy–Chapman model (3.5), one arrives at the Poisson–Boltzmann system [BF80]:

$$-\nabla \varepsilon_0 \varepsilon_r \nabla \phi = Fc \sum_{\alpha=1}^{N-1} z_\alpha \exp\left(\frac{z_\alpha F}{RT}(\psi_\alpha - \phi)\right). \tag{3.15}$$

For the Bikerman–Freise model (3.7), a generalised Poisson–Boltzmann equation arises:

$$-\nabla\varepsilon_0\varepsilon_r\nabla\phi = F\bar{c}\sum_{\alpha=1}^{N-1}\frac{z_\alpha\exp\left(\frac{z_\alpha F}{RT}(\psi_\alpha-\phi)\right)}{a_\alpha^\circ\left(1+\sum_{i=1}^{N-1}\frac{1}{a_i^\circ}\exp\left(\frac{z_i F}{RT}(\psi_i-\phi)\right)\right)}. \tag{3.16}$$

In the case of equal reference activities, all inverses activity coefficients $\beta_\alpha^{\mathrm{BF}}$ are equal, and (3.16) simplifies to

$$-\nabla\varepsilon_0\varepsilon_r\nabla\phi = F\bar{c}\frac{\sum_{\alpha=1}^{N-1}z_\alpha\exp\left(\frac{z_\alpha F}{RT}(\psi_\alpha-\phi)\right)}{a^\circ+\sum_{\alpha=1}^{N-1}\exp\left(\frac{z_\alpha F}{RT}(\psi_\alpha-\phi)\right)} \tag{3.17}$$

For $a^\circ = 1$ and $N-1=2$, this equation has been stated already in [Bik42].
For the pressure correction model, a system of two coupled partial differential equations arises:

$$-\nabla\varepsilon_0\varepsilon_r\nabla\phi = \bar{c}\exp\left(-\frac{p-p^\circ}{\bar{c}RT}\right)F\sum_{\alpha=1}^{N-1}\frac{z_\alpha}{a_\alpha^\circ}\exp\left(\frac{z_\alpha F}{RT}(\psi_\alpha-\phi)\right) \tag{3.18a}$$

$$\Delta p = -\nabla\cdot q\nabla\phi \tag{3.18b}$$

According to lemma 2.1, equation (3.18a) can be replaced by equation (3.16), leading to a significant decoupling. In particular, the potential can be determined independent of the pressure, and it is sufficient to solve the pressure equation only if there is interest in the pressure itself.

3.5.1. *Fermi–Dirac model.* In this case, by definition, the exponential function which is representing the Boltzmann statistics in (3.15) is replaced by the Fermi integral:

$$-\nabla\varepsilon_0\varepsilon_r\nabla\phi = F\bar{c}\sum_{\alpha=1}^{N-1}z_\alpha\mathcal{G}\left(\frac{z_\alpha F}{RT}(\psi_\alpha-\phi)\right) \tag{3.19}$$

$$\overset{\mathcal{G}=\mathcal{F}_{-1}}{=} F\bar{c}\sum_{\alpha=1}^{N-1}\frac{z_\alpha}{a_\alpha^\circ+\exp\left(\frac{z_\alpha F}{RT}(\phi-\psi_\alpha)\right)} \tag{3.20}$$

$$= F\bar{c}\sum_{\alpha=1}^{N-1}\frac{z_\alpha\exp\left(\frac{z_\alpha F}{RT}(\psi_\alpha-\phi)\right)}{a_\alpha^\circ+\exp\left(\frac{z_\alpha F}{RT}(\psi_\alpha-\phi)\right)}. \tag{3.21}$$

Again, one observes the simplification of the Bikerman–Freise model (3.16).

4. Finite volume schemes consistent with thermodynamical equilibrium

This section discusses numerical schemes with respect to their qualitative properties, in particular consistency to the thermodynamical equilibrium. This means that the discrete equivalent of the zero flux condition is consistent with the expression

$$c_\alpha = \bar{c}\beta_\alpha a_\alpha = \bar{c}\beta_\alpha\exp\left(\frac{z_\alpha F}{RT}(\psi_\alpha-\phi)\right) \tag{4.1}$$

where ϕ is a given value of the electrostatic potential and ψ_α is the constant quasi-Fermi potential of species α. In the sequel, in this section, $Z_\alpha = \frac{z_\alpha F}{RT}$ and the index α is will be omitted.

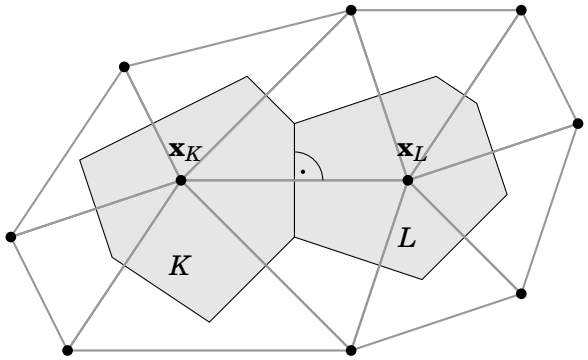

FIGURE 3.1. Collocation points (black), simplices (grey lines) and control volumes (filled) in two space dimensions. Note the right angle between the lines $\mathbf{x}_K\mathbf{x}_L$ and $\partial K \cap \partial L$.

4.1. **General description of the scheme.** What follows, is a short description of the Voronoï box based finite volume method [Mac53], known also as "box method" [BR87] or "control volume method". Due to its unique properties [GG09, SGF10], it is the method of choice in the field of semiconductor device simulation and others, where positivity of solutions, maximum principles and consistency to thermodynamical laws are of significant. The definition of the method as well fits to the definition of an admissible grid in [EGH00], giving rise to the possibility to apply compactness based convergence analysis tools.

This discretization is based on a subdivision of the calculation domain Ω into a finite number of open, polygonal control volumes K around the collocation points $\mathbf{x}_K$. Such a control volume subdivision can be obtained by using a triangular or tetrahedral grid. For this grid, one requires the boundary-conforming Delaunay property [SGF10]. This means that for any given simplex of the grid, the interior of the ball spanned by its vertices does not contain any vertex of any other simplex, and that its circumcenter is located in the interior of the domain Ω or at its boundary. In two space dimensions, the mesh generator triangle [She] is able to create this type of grids. In three space dimension, with some restrictions, TetGen [Si14] allows to create this type of meshes.

The Delaunay property allows to obtain the control volumes surrounding each given collocation point by joining the circumcenters of the simplices adjacent to it (Fig. 3.1). It is important to note that for two neighbouring control volumes, the grid edge $\mathbf{x}_L\mathbf{x}_K$ is orthogonal to the face separating the control volumes.

Denote by ∂K the boundary of the control volume K, and by $|\xi|$, the measure (volume, surface, length) of a geometrical object ξ. For each space-time control volume $K \times (t^{n-1}, t^n)$, integrate the continuity equation (2.1) and apply the Gauss theorem to the integral of the flux divergence:

$$
\begin{aligned}
0 =& \frac{1}{t^n - t^{n-1}} \int_{t^{n-1}}^{t^n} \int_K (\partial_t c + \nabla \cdot \mathbf{N})\, d\mathbf{x}\, dt \\
=& \frac{1}{t^n - t^{n-1}} \left(\int_{t^{n-1}}^{t^n} \int_K \partial_t c \; d\mathbf{x} dt + \int_{t^{n-1}}^{t^n} \int_{\partial K} \mathbf{N} \cdot \mathbf{n} \; ds \right) \\
=& \int_K \frac{c^n - c^{n-1}}{t^n - t^{n-1}} \; d\mathbf{x} dt + \frac{1}{t^n - t^{n-1}} \sum_{L \text{ neighbour of } K} \int_{t^{n-1}}^{t^n} \int_{\partial K \cap \partial L} \mathbf{N} \cdot \mathbf{n}_{KL} ds \\
\approx& |K| \frac{c_K^n - c_K^{n-1}}{t^n - t^{n-1}} + \sum_{L \text{ neighbour of } K} |\partial K \cap \partial L| N_{KL}^n
\end{aligned}
\tag{4.2}
$$

In a similar manner, one obtains for the Poisson equation

$$
\sum_{L \text{ neighbour of } K} |\partial K \cap \partial L| E_{KL}^n = |K| q_K^n. \tag{4.3}
$$

Here, c_K^n, q_K^n are the values of the concentration and the charge in the collocation point $\mathbf{x}_K$ at moment t^n, respectively. N_{KL}^n and E_{KL}^n are the respective averaged projections of the molar flux and the electric field onto the normal directions of the Voronoi box faces $\partial K \cap \partial L$. By the orthogonality property described above, these normal directions are aligned with the directions of the the simplex edges. As a consequence, N_{KL}^n and E_{KL}^n can be expressed consistently by the unknown values in the collocation points $\mathbf{x}_K$ and $\mathbf{x}_L$. Aiming at the unconditional stability of the scheme, these unknown values are chosen solely from the moment t^n.
In a straightforward manner, the electric field projection can be expressed by the finite difference expression

$$
E_{KL}^n = \varepsilon \varepsilon_0 \frac{\phi_K^n - \phi_L^n}{|\mathbf{x}_K - \mathbf{x}_L|}. \tag{4.4}
$$

Denoting by p_K^n the pressure in the collocation point $\mathbf{x}_K$ and moment t^n, and $q_{KL}^n = \frac{1}{2}(q_K^n + q_L^n)$, the momentum balance can be discretized as

$$
\sum_{L \text{ neighbour of } K} |\partial K \cap \partial L| \frac{p_K^n - p_L^n}{|\mathbf{x}_K - \mathbf{x}_L|} = \sum_{L \text{ neighbour of } K} |\partial K \cap \partial L| q_{KL}^n \frac{\phi_K^n - \phi_L^n}{|\mathbf{x}_K - \mathbf{x}_L|}. \tag{4.5}
$$

One should note that these notations for the discretization hold for all space dimensions including allowing for a dimension-independent implementation of the method.

4.2. **Consistency to thermodynamical equilibrium.** In the thermodynamical equilibrium, it is straightforward to chose the value of q_K by inserting $\phi = \phi_K$ into the different right hand side expressions from section 3.5. A thermodynamically correct approximation N_{KL}^n should be consistent to this choice [BC12].
The discussion of this issue starts with the classical Nernst–Planck case $\beta_\alpha = 1$. For the thermodynamical equilibrium value one has $c_= = \bar{c} \exp(Z(\psi - \phi))$ with a constant quasi-Fermi potential ψ and a position dependent electrostatic potential ϕ. Correspondingly, in the numerical scheme, one has $c_{=,K} = \bar{c} \exp\big(Z(\psi - \phi_K)\big)$. Consistency of the time dependent scheme to the thermodynamical equilibrium

means that for such values of $c_{=,K}$, the resulting numerical flux N_{KL} is zero. In the discussed case, the well known Scharfetter-Gummel scheme [SG69]

$$N_{KL} = D\left(B(Z(\phi_L - \phi_K))c_K - B(Z(\phi_K - \phi_L))c_L\right) \tag{4.6}$$

is the approximation of choice. Here, $B(\xi) = \frac{\xi}{\exp(\xi)-1}$ is the Bernoulli function. It has been derived from solving a two point boundary value problem at the discretization edge emerging from the projection of the flux expression (see also [EFG06]).

Lemma 4.1. *The Scharfetter-Gummel scheme* (4.6) *is consistent to the thermodynamical equilibrium.*

Proof. For any given constant value of ψ, assuming $N_{KL} = 0$ (4.6) leads to

$$\frac{c_K}{c_L} = \frac{B(Z(\phi_K - \phi_L))}{B(Z(\phi_L - \phi_K))} = -\frac{\exp(Z(\phi_L - \phi_K)) - 1}{\exp(Z(\phi_K - \phi_L)) - 1} \tag{4.7}$$

$$= -\frac{\exp(Z\phi_L)}{\exp(Z\phi_K)} \cdot \frac{\exp(-Z\phi_K) - \exp(-Z\phi_L)}{\exp(-Z\phi_L) - \exp(-Z\phi_K)} \tag{4.8}$$

$$= \frac{\exp(Z\phi_L)}{\exp(Z\phi_K)} = \frac{\exp(Z(\psi - \phi_K))}{\exp(Z(\psi - \phi_L))} \tag{4.9}$$

$$= \frac{c_{=,K}}{c_{=,L}} \tag{4.10}$$

□

After observing that the flux in the activity based formulation up to the prefactor $\bar{c}\beta$ has the same structure as the uncorrected concentration flux in the classical Nernst–Planck system, one can propose the ansatz

$$N_{KL} = \bar{c}D\overline{\beta}(B(Z(\phi_L - \phi_K))a_K - B(Z(\phi_K - \phi_L))a_L). \tag{4.11}$$

where $\overline{\beta}$ is some mean of β on $[a_K, a_L]$.

Lemma 4.2. *For any mean $\overline{\beta}$ of β on $[a_K, a_L]$, the flux discretization* (4.11) *is consistent to the thermodynamical equilibrium.*

Proof. Setting $N_{KL} = 0$ in (4.11) yields

$$\frac{a_K}{a_L} = \frac{\exp(Z(\psi - \phi_K))}{\exp(Z(\psi - \phi_L))}. \tag{4.12}$$

But this is consistent with the expression for a in (4.1) resulting in a similarly consistent expression for $c = \beta a$. □

Thus, the consistency to thermodynamical equilibrium is a condition on the activity flux discretization which is independent on the averaging of the inverse activity coefficient β.

4.3. **Numerical examples.** All subsequent examples are solved numerically using the described finite volume method implemented for shared memory parallel machines within the framework of pdelib [SF+14]. The nonlinear equations resulting form the implicit discretization scheme are solved using Newton's method. The linear systems are solved using the direct solver Pardiso [SGK+14]. Due to the complexities connected with the solution of the nonlinear system (3.9) at each discretization point, results will be presented for the Gouy–Chapman model (2.9),

the Bikerman–Freise-Model (2.13), the pressure correction model (2.19), and the Fermi–Dirac model (2.24).
Most likely, the proposed activity based approach will work as well in the general case of (3.10) and corresponding extensions which include solvation effects [DGL14]. The investigation of this situation will be the subject of a followup paper.

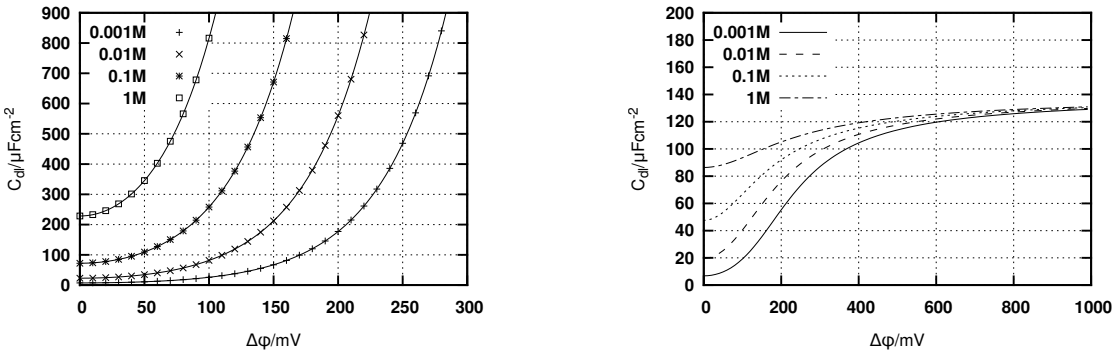

FIGURE 4.1. Left: Double layer capacity curves according to the Gouy–Chapman model — numerical solution (points) vs. exact value (4.15) (lines). Right: Gouy–Chapman-Stern model (OHP at $x = 0.5\,\mathrm{nm}$) — numerical solution for an aqueous 1:1 electrolyte at 25°C matching the results in [BF80].

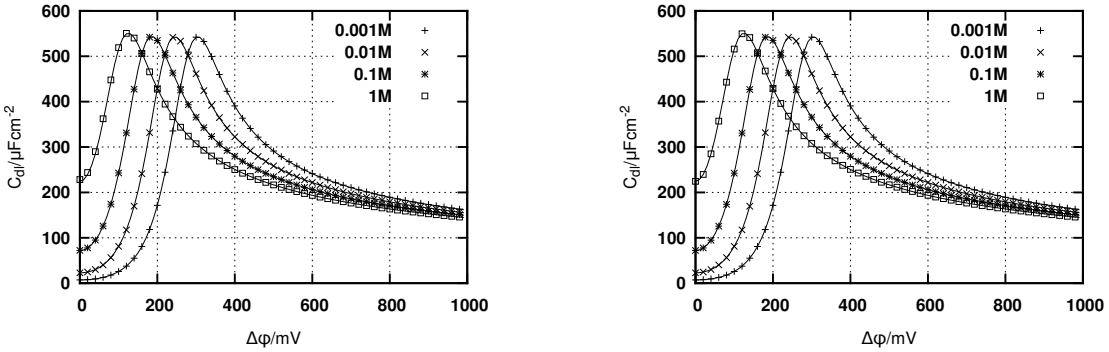

FIGURE 4.2. Comparison of the differential double layer capacitance curves between the Bikerman–Freise model (3.16) (lines) and the pressure correction model (3.18) (points; left) resp. the Fermi–Dirac model of index -1 (3.21) (points; right).

4.3.1. *Differential double layer capacitance for a symmetric* $1:1$ *electrolyte.* Regard system (3.13) in the one-dimensional domain $\Omega = (0,L)$. Assume the following boundary conditions:

$$\phi|_{x=0} = \phi_0, \qquad \phi|_{x=L} = \phi_\infty, \tag{4.13a}$$

$$-\nabla p \cdot \mathbf{n}|_{x=0} = q\nabla\phi \cdot \mathbf{n}|_{x=0}, \qquad p|_{x=L} = p_\infty. \tag{4.13b}$$

The quasi-Fermi potentials are obtained from given concentration values $c_\alpha|_{x=L} = c_{\alpha,\infty} << \bar{c}$ such that $q|_{x=L} = F\sum_{\alpha=1}^{N-1} z_\alpha c_{\alpha,\infty} = 0$. Further, set $p^\circ = 0$.
More specifically, regard a symmetric electrolyte with $z_1 = 1, z_2 = -1$ and a given molarity of the bulk solution $c_{\alpha,\infty} = c_\infty$ for $\alpha = 1,2$. The summary concentration $\bar{c}$

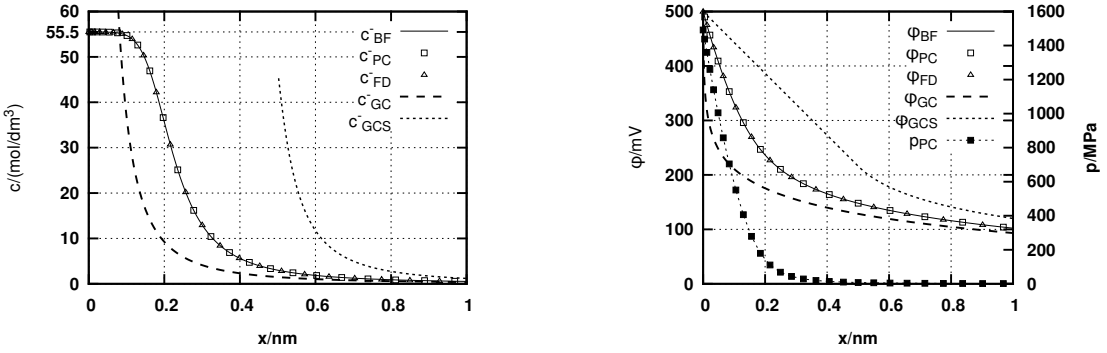

FIGURE 4.3. 500 mV applied potential and 0.01 mol/dm^3 1:1 electrolyte concentration. Left: negative ion concentrations for the different models. Right: pressure (for the pressure correction model) and electrostatic potential for the different models.

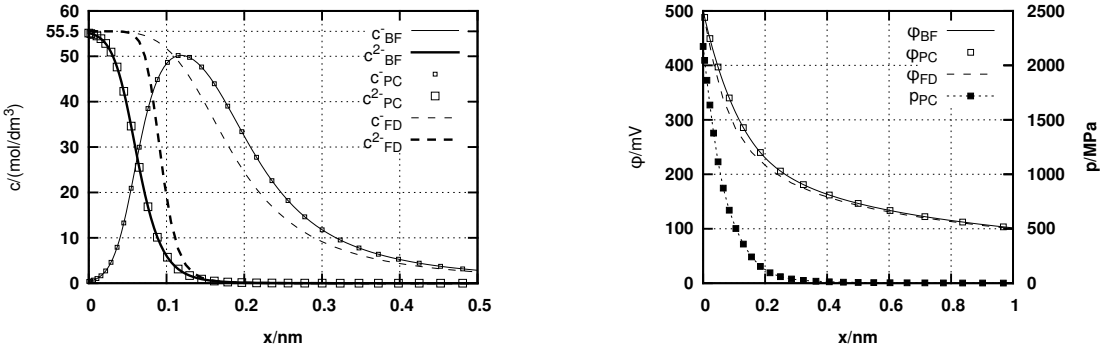

FIGURE 4.4. Ternary electrolyte with 500 mV applied potential, 0.01 mol/dm^3 bulk positive ion concentration. Left: negative ion concentrations. Right: electrostatic potential and pressure.

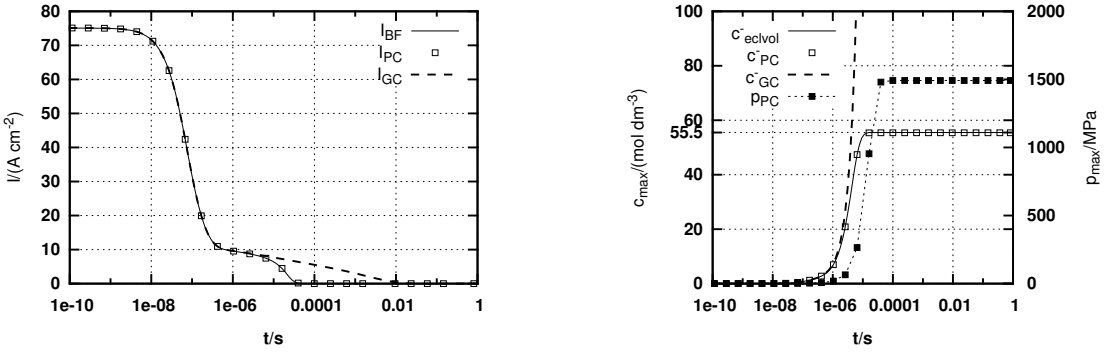

FIGURE 4.5. Evolution of current (left) and maximum negative ion concentration (right).

is set to the molarity of water $\bar{c} = 55.508\,\mathrm{mol/dm^3}$. In the Gouy–Chapman case, the Poisson–Boltzmann equation (3.15) with $\beta_\alpha^{\mathrm{GC}} = 1$ yields an exact solution [BF80]

$$\phi(x) = \frac{RT}{4F}\,\mathrm{atanh}\left(\tanh\left(\phi_0\frac{F}{4RT}\right)\exp\left(-\frac{x}{\lambda_D}\right)\right). \tag{4.14}$$

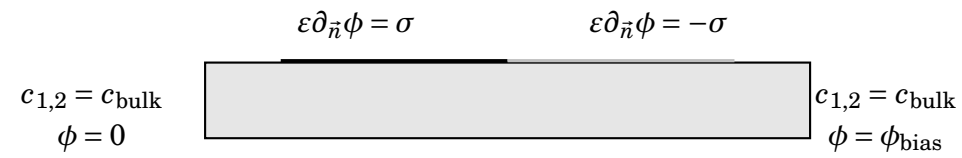

FIGURE 4.6. Electrolytic diode in a nanopore. If not stated otherwise: $\partial_{\vec{n}}\phi = 0$, $\partial_{\vec{n}}p = 0$, $\vec{N}_{1,2}\cdot\vec{n} = 0$, $\sigma = 85\,\mu\text{As/m}^2$, $c_{\text{bulk}} = 2$ mol/dm^3. Pore length =100 nm, pore width=2, 4, 8 nm

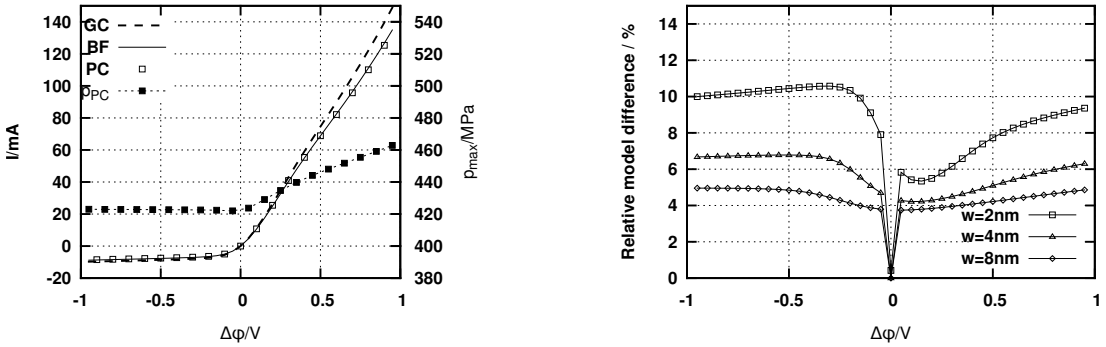

FIGURE 4.7. Left: IV-Curves for the different models (pore width $= 2\ nm$). Right: discrepancy between the models for different pore widths.

Here $\lambda_D = \sqrt{\frac{\varepsilon_0\varepsilon_r RT}{2F^2 c_\infty}}$ is the Debye length, which describes the characteristic size of the diffusive boundary layer. The charge stored in the system – concentrated in the boundary layer – can be calculated from $Q_{dl} = Q_{dl}(\phi_0) = \int_0^L q\ dx$. For the differential double layer capacitance C_{dl} one obtains [BF80]:

$$C_{dl} := \frac{dQ_{dl}}{d\phi_0} = \sqrt{\frac{2\varepsilon_0\varepsilon_r F^2 c_\infty}{RT}}\cosh\left(\frac{\phi_0 F}{2RT}\right) \tag{4.15}$$

The numerical calculations have been performed using a grid of 1024 nodes with geometric point distribution providing local grid refinement towards the electrode at $x = 0$. The double layer capacitance is calculated numerically using the finite difference of double layer charges for two close values of ϕ_0. The double layer capacitance curves representing the Gouy–Chapman model (4.15) in fig. 4.1 (left) are recovered with high accuracy along with known values of the double layer capacitance, e.g. for $c_\infty^\pm = 0.01\,\text{mol/dm}^3$, $C_{dl} = 22.8\,\mu\text{F/cm}^2$ for $\phi_0 = 0\,\text{V}$ [BF80].
The Gouy–Chapman-Stern model [Ste24, BF80] introduces the outer Helmholtz plane (OHP) at a distance of an ion radius from the electrode. Between the electrode and the OHP, the space charge is assumed to be zero, and the Poisson equation is solved. Outside of the OHP, the Poisson–Boltzmann equation (3.15) is valid. This model leads to a significant limitation of the predicted double layer capacitance, as can be seen e.g. from figure 4.1 (right). On the other hand, this model misses the fact that experimental data show a decrease of the differential double layer capacitance with larger potential differences [BF80].
In fig. 4.3 (left), the curves of the differential double layer capacitance's for the Bikerman–Freise model (2.13), (3.16) and the pressure correction model (2.19), (3.18)

are plotted. As predicted in lemma 2.1, an exact match between both models is observed, though indeed the numerical calculations have been performed for the corresponding different systems (3.16) resp. (3.18).
In fig. 4.3 (right), the curves of the differential double layer capacitance for Bikerman–Freise model (2.13), (3.16) and the Fermi–Dirac model (2.24), (3.21) are plotted. They as well exhibit a nearly perfect match. Close to the electrode the positive ion activity becomes very small, therefore its influence becomes negligible an one obtains $\beta_2^{\mathrm{BF}} \approx \beta_2^{\mathrm{FD}}$.
A similar match between the Bikerman–Freise (3.16), pressure correction (3.18), and Fermi–Dirac models (3.21) for the negative ion concentration profile for an ion concentration $c_\infty^\pm = 0.01\,\mathrm{mol/dm^3}$ and an applied voltage of $\phi_0 = 0.5\,\mathrm{V}$. is observed close to the electrode in fig. 4.3 (left). All three models limit the concentration in the boundary layer to the summary concentration $\bar{c}$. For comparison, the corresponding profiles for the Gouy–Chapman (3.15) and the Gouy–Chapman-Stern models have been added to the plot.
Fig 4.3 (right) demonstrates the different distributions of the electrostatic potential. For the pressure correction model (3.18), the profile of the pressure has been added. The maximum value of the pressure of 1491.5 MPa appears to be very high. However, the authors of [DGM13] estimate a maximum pressure of $\approx 200\,\mathrm{MPa}$ for an applied potential of $\approx 300\,\mathrm{mV}$ in the case of an asymmetric electrolyte. For an applied potential of $\approx 300\,\mathrm{mV}$, the model in the present paper yields a maximum pressure of 427 MPa which lies in the same order of magnitude.

4.3.2. *Ternary electrolyte.* The implementation of the numerical model has been realised for an arbitrary number of ionic species. Fig. 4.4 demonstrates the results of calculations for a ternary electrolyte with $z_1 = 1, z_2 = -1, z_3 = -2$. The bulk ion concentrations are $c_1 = 0.01\,\mathrm{mol/dm^3}, c_2 = (0.01 - 10^{-8})\,\mathrm{mol/dm^3}, c_3 = 5 \cdot 10^{-9}\,\mathrm{mol/dm^3}$. There is a stronger attraction of the doubly charged ions to the electrode. Therefore, with approximately equal bulk concentrations, the double layer would nearly exclusively contain doubly charged negative ions. However, due to the small bulk concentration of the doubly charged ions, they are not able to fill the boundary layer completely, and additional singly charged ions have to be taken to fill it up. This explains the maximum of the singly charged ion concentration in a certain distance to the boundary. Both the pressure correction and the Bikerman–Freise models catch this effect very well. The resulting concentrations are in the relevant physical limits. The Fermi–Dirac model however ignores the competition between the two negative ion species. This leads to an unphysical summary concentration of negative ions (both concentrations reach the limit of $55.5\,\mathrm{mol/dm^3}$separately). Moreover, the maximum of the singly charged ion concentration at a distance to the electrode is completely missed.

4.3.3. *Dynamic Nernst–Planck calculations.* Setting in addition to the previous data $D_\alpha = 10^{-9}\mathrm{m^2/s}$, the evolution of the voltage and concentration profile is calculated by the Nernst–Planck equations using different models. The molar masses M_α and M_N are assumed to be equal.
Both the Bikerman–Freise model – which in this case is equivalent to the complete model of an incompressible ideal mixture according to [DGM13] (2.17) – and the pressure correction model give nearly the same result. In comparison to the Gouy–Chapman model, the charging time for the double layer is at least two orders of

magnitude shorter. This of course can be explained by the fact that significantly more charge has to be transported into a Gouy–Chapman layer.
Tests for bot the binary and the ternary electrolyte confirmed that the in the large time limit, the result of the Nernst–Planck calculations matches that of the equilibrium calculations.

4.3.4. *Electrolytic diode.* The models are applied in a 2D situation representing an electrolytic diode in a nano-channel filled with a binary 1:1 electrolyte (fig. 4.3). Fig. 4.3 (left) presents an I-V curve which exhibits the behaviour of a diode. In difference to a semiconductor diode, the current is an ionic current, and the fixed surface charge $\pm\sigma$ plays the role of the doping. Fig. 4.3 as well demonstrates the influence of the model discrepancy on the I-V curve. In particular, the influence of the model error decreases with the pore width. The maximum pressure value is in the same order of magnitude as the values estimated in [EB11] for the case of a nanopore in a polymer electrolyte membrane.

Acknowledgement

The author is thankful for numerous, sometimes intense discussions with the colleagues at WIAS, namely W. Dreyer, K. Gärtner, J. Griepentrog, C. Guhlke, Th. Koprucki and M. Landstorfer. This work was carried out in the framework of the project “Macroscopic Modeling of Transport and Reaction Processes in Magnesium-Air-Batteries” (Grant 03EK3027D) under the research initiative “Energy storage” of the German Federal government.

Appendix A. Notations

Constants		
e	$1.602\cdot10^{-19}$ As	elementary charge
ε_0	$8.85\cdot10^{-12}$ F/m	dielectric permittivity of vacuum
$F = N_A e$	$9.65\cdot10^{4}$ As/mol	Faraday constant
k	$1.381\cdot10^{-23}$ J/K	Boltzmann constant
N_A	$6.022\cdot10^{23}$ mol^{-1}	Avogadro constant
$R = kN_A$	8.314 J/(mol K)	Gas constant

Species properties		
$c_\alpha = n_\alpha/N_A$	mol/m^3	molar density (concentration)
m_α	kg	molecular mass
g°_α	J/kg	specific reference Gibbs energy
$M_\alpha = m_\alpha N_A$	kg/mol	molar mass
μ°_α	J/mol	reference chemical potential
n_α	1/m^3	number density
$\mathbf{N}_\alpha = c_\alpha v_\alpha$	mol/(m^2 s)	molar flux
$\rho_\alpha = m_\alpha n_\alpha = M_\alpha c_\alpha$	kg/m^3	mass density
$\mathbf{v}_\alpha$	m/s	velocity
z_α	1	charge number

Mixture properties		
$\bar{c} = \sum_{\alpha=1}^{N} c_\alpha = n/N_A$	$\mathrm{mol/m^3}$	summary molar density
ε_r	1	rel. dielectric permittivity
η	Pa s	viscosity
K	Pa	bulk modulus
$L_{\alpha\beta}$	$\mathrm{kg\,K\,s/m^3}$	Onsager coefficients
λ_D	m	Debye length
$n = \sum_{\alpha=1}^{N} n_\alpha$	$1/\mathrm{m^3}$	summary number density
n°	Pa	reference number density
p	Pa	pressure
p°	Pa	reference pressure
ϕ	V	electrostatic potential
$q = e\sum_{\alpha=1}^{N} z_\alpha n_\alpha = F\sum_{\alpha=1}^{N} z_\alpha c_\alpha$	$\mathrm{As/m^3}$	space charge density
$\rho = \sum_{\alpha=1}^{N} \rho_\alpha$	$\mathrm{kg/m^3}$	mass density
$\mathbf{v} = \frac{1}{\rho}\sum_{\alpha=1}^{N} \rho_\alpha \mathbf{v}_\alpha$	m/s	barycentric velocity

Species properties relative to mixture		
a_α	1	activity
β_α	1	inverse activity coefficient
$D_\alpha = \frac{L_{\alpha\alpha}R}{M_\alpha^2 c_\alpha}$	$\mathrm{m^2/s}$	diffusion coefficient
$g_\alpha = \frac{\partial U}{\partial \rho_\alpha}$	J/kg	specific Gibbs energy of species
γ_α	1	activity coefficient
$\mathbf{J}_\alpha = \rho_\alpha(\mathbf{v}_\alpha - \mathbf{v})$	$\mathrm{kg/(m^2 s)}$	non-convective mass flux
$\mu_\alpha = \frac{\partial U}{\partial c_\alpha} = M_\alpha g_\alpha$	J/mol	chemical potential
$\tilde{\mu}_\alpha = \mu_\alpha - \frac{M_\alpha}{M_N}$	J/mol	effective chemical potential
$\mathbf{N}_\alpha = c_\alpha(\mathbf{v}_\alpha - \mathbf{v})$	$\mathrm{mol/(m^2 s)}$	non-convective molar flux
ψ_α	V	quasi-Fermi potential
v_α	$\mathrm{m^3/mol}$	partial molar volume
$y_\alpha = n_\alpha/n = c_\alpha/c$	1	molar fractions

Appendix B. Generalised Nernst–Planck–Poisson model according to [DGM13]

B.1. **Compressible case.** The proposed model for an ionic fluid mixture of N constituents (with viscosity terms added and polarisation effects omitted) has unknowns $\phi, n_\alpha (\alpha = 1 \ldots N-1), \mathbf{v}$. The Nth component is assumed to be the solvent. The model reads as follows:

$$\partial_t \rho + \nabla\cdot(\rho\mathbf{v}) = 0 \tag{B.1a}$$

$$\partial_t \rho_\alpha + \nabla\cdot(\rho_\alpha\mathbf{v} + \mathbf{J}_\alpha) = 0, \quad \alpha = 1\ldots N-1 \tag{B.1b}$$

$$\partial_t(\rho\mathbf{v}) + \nabla\cdot(\rho\mathbf{v}\otimes\mathbf{v}) - \eta\Delta\mathbf{v} + \nabla p = -q\nabla\phi \tag{B.1c}$$

$$-\nabla\cdot\varepsilon_0\varepsilon_r\nabla\phi = q. \tag{B.1d}$$

The following notations have been changed compared to [DGM13]: $n^F \to q$, $z_\alpha \to e z_\alpha$, $\mu_\alpha \to g_\alpha$, $1+\chi \to \varepsilon_r$. $\cdot^R \to \cdot^\circ$.

Citing [dGM62, Mü85], the authors provide the following expression for the diffusive fluxes:

$$\mathbf{J}_\alpha = -\sum_{\beta=1}^{N-1} L_{\alpha\beta}\left(\nabla\left(\frac{g_\beta - g_N}{T}\right) + \frac{1}{T}\left(\frac{ez_\beta}{m_\beta} - \frac{ez_N}{m_N}\right)\nabla\phi\right) \qquad (\alpha = 1\ldots N-1). \tag{B.1e}$$

The following constitutive relationships for the chemical potentials and the pressure are proposed:

$$g_\alpha = g_\alpha^\circ + \frac{K}{m_\alpha n^\circ}\ln\left(1 - \frac{p-p^\circ}{K}\right) + \frac{kT}{m_\alpha}\ln y_\alpha \qquad (\alpha = 1\ldots N) \tag{B.1f}$$

$$p = p^\circ + K\left(\frac{n}{n^\circ} - 1\right). \tag{B.1g}$$

B.2. **Incompressible case.** Incompressibility is equivalent to obtaining the limit $K \to \infty$. Repeating the calculations given in [DGM13] for the one-dimensional equilibrium case, the constitutive equation for the density is re-arranged:

$$\frac{n}{n^\circ} = 1 + \frac{p-p^\circ}{K} \tag{B.2}$$

Then, the limit of (B.1f), (B.1g) for $K \to \infty$ is

$$g_\alpha = g_\alpha^\circ + \frac{1}{m_\alpha n^\circ}(p-p^\circ) + \frac{kT}{m_\alpha}\ln y_\alpha \qquad (\alpha = 1\ldots N) \tag{B.3}$$

$$n = n^\circ \tag{B.4}$$

B.3. **Transformation to molar based quantities, isothermal case.** In order to be consistent with the electrochemical literature, the system is transformed to molar quantities, at the same time assuming constant temperature. This amounts to replace the number density by the molar density (concentration), and the specific Gibbs energy g_α (in [DGM13] referred to as chemical potential μ_α) by the molar chemical potential $\mu_\alpha = \frac{g_\alpha}{M_\alpha}$. In order to be consistent with the momentum balance in the Navier–Stokes equations one has to define diffusion with respect to the barycentric velocity rather the molar average velocity, an option discussed e.g. in [dGM62]. Therefore the transformation is just a change of variables.
One notes

$$c_N = \bar{c} - \sum_{\alpha=1}^{N-1} c_\alpha \tag{B.5a}$$

$$\rho = \sum_{\alpha=1}^{N} M_\alpha c_\alpha = M_N\left(c - \sum_{\alpha=1}^{N-1} c_\alpha\right) + \sum_{\alpha=1}^{N-1} M_\alpha c_\alpha \tag{B.5b}$$

$$= M_N\bar{c} + \sum_{\alpha=1}^{N-1}(M_\alpha - M_N)c_\alpha. \tag{B.5c}$$

Transformation to mole based quantities and the isothermal case results in the Navier–Stokes System (2.5), the Poisson equation (2.1a), the mass conservation equation (2.1b), and the flux expression

$$\mathbf{N}_\alpha = -\sum_{\beta=1}^{N-1} \frac{L_{\alpha\beta}}{TM_\alpha}\left(\nabla\left(\frac{\mu_\beta}{M_\beta} - \frac{\mu_N}{M_N}\right) + \left(\frac{z_\beta F}{M_\beta} - \frac{z_N F}{M_N}\right)\nabla\phi\right) \qquad (\alpha = 1\ldots N-1). \tag{B.6}$$

The constitutive relationship for the chemical potential (B.3) transforms to (2.14).

B.4. **Diagonalisation of fluxes.** For the considerations in this paper the following common assumptions are made:

$$z_N = 0, \qquad \text{(neutral solvent)} \tag{B.7a}$$

$$L_{\alpha\beta} = 0, \alpha \neq \beta, \qquad \text{(diagonal Onsager coefficients)} \tag{B.7b}$$

$$L_{\alpha\alpha} = M_\alpha^2 T D_\alpha c_\alpha \qquad \text{(relation between Onsager and Fickian diffusion coefficient).} \tag{B.7c}$$

As a result, (B.6) turns into the Nernst–Planck equation (2.1c).

Appendix C. Concentration based formulations

Concentration based formulations of solute transport are widely familiar. Therefore, in this appendix, the consequences of reformulation of the Nernst Planck system using concentrations as basic unknowns are discussed.

C.1. **Gouy–Chapman model.** For the chemical potential defined in (2.9) one obtains

$$c_\alpha = c \exp\left(\frac{\tilde{\mu}_\alpha - \tilde{\mu}_\alpha^\circ}{RT}\right)$$

and re-establishes the classical Nernst–Planck flux as described e.g. in [NTA12]:

$$\mathbf{N}_\alpha = -D_\alpha \left(\nabla c_\alpha + \frac{z_\alpha F}{RT} c_\alpha \nabla \phi\right) \qquad (\alpha = 1 \ldots N-1). \tag{C.1}$$

C.2. **Bikerman–Freise model.** For the chemical potential defined in (2.13), one obtains

$$\begin{aligned} \frac{D_\alpha}{RT} c_\alpha \nabla \tilde{\mu}_\alpha &= D_\alpha \nabla c_\alpha - D_\alpha c_\alpha \left(1 - \sum_{\beta=1}^{N-1} \frac{c_\beta}{\bar{c}}\right) \sum_{\beta=1}^{N-1} \nabla \frac{c_\beta}{\bar{c}} \qquad (\alpha = 1 \ldots N-1), \\ \mathbf{N}_\alpha &= D_\alpha \left(\nabla c_\alpha - c_\alpha \left(1 - \sum_{\beta=1}^{N-1} \frac{c_\beta}{\bar{c}}\right) \sum_{\beta=1}^{N-1} \nabla \frac{c_\beta}{\bar{c}} - c_\alpha z_\alpha \frac{F}{RT} \nabla \phi\right) \quad (\alpha = 1 \ldots N-1). \end{aligned} \tag{C.2}$$

This expression couples all concentration gradients in the system, providing quite significant challenges for analytical and numerical treatment. Moreover, the expression of the thermodynamical equilibrium is hard to obtain.

C.3. **Incompressible ideal mixture.** In order to make the main point here, the model of [DGM13] can be discussed first in the limit case (according to lemma 2.1) of the Bikerman–Freise model, where all objections discussed for (C.2) apply.
In the limit case of pressure correction (2.19), one obtains $\nabla \tilde{\mu}_\alpha = \frac{1}{\bar{c}} \nabla p + RT \frac{1}{c_\alpha} \nabla c_\alpha$ resulting in the flux expression

$$\mathbf{N}_\alpha = -D_\alpha \left(\nabla c_\alpha + \frac{1}{\bar{c} RT} c_\alpha \nabla p + \frac{z_\alpha F}{RT} c_\alpha \nabla \phi\right), \qquad (\alpha = 1 \ldots N-1). \tag{C.3}$$

The additional effect from the pressure gradient is sometimes called *barodiffusion*. In the context of (electroneutral) liquid mixture theory, it has been discussed in [LL86] as a consequence of the general assumption that the chemical potential is allowed to depend on the pressure.
The regularity theory for weak solutions of the incompressible Navier-Stokes equations predicts poor regularity of the pressure. Thus, in general, the notation of a

pressure gradient is not well defined, and one has to expect difficulties in obtaining convergence results for numerical schemes based on this approach.
In the mechanical equilibrium, the situation is slightly better, as the pressure gradient can be related to the electrostatic potential gradient via (2.7). On can use this relationship to exclude the pressure from the system (C.3) and arrives at

$$\mathbf{N}_\alpha = -D_\alpha \left(\nabla c_\alpha + \frac{z_\alpha F - \frac{q}{\bar{c}}}{RT} c_\alpha \nabla \phi \right) \tag{C.4}$$

yielding a similar term as in [Rou06].

C.4. **Fermi–Dirac model.** First, from (2.21), and the differentiation rule for inverse functions one obtains

$$\tilde{\mu}_\alpha(c_\alpha) = \tilde{\mu}_\alpha^\circ + RT \mathscr{G}^{-1}\left(\frac{c_\alpha}{\bar{c}}\right) \tag{C.5}$$

$$\nabla \tilde{\mu}_\alpha(c_\alpha) = \frac{RT}{\bar{c}} \mu_\alpha'(c_\alpha) \nabla c_\alpha = \frac{RT}{\bar{c}} \frac{1}{\mathscr{G}'\left(\mathscr{G}^{-1}\left(\frac{c_\alpha}{\bar{c}}\right)\right)} \nabla c_\alpha \tag{C.6}$$

The Nernst–Planck flux rewrites as

$$\begin{aligned} \mathbf{N}_\alpha = -\frac{D_\alpha}{RT} c_\alpha \left(\nabla \tilde{\mu}_\alpha + z_\alpha F \nabla \phi \right) &= -\frac{D_\alpha}{RT} c_\alpha \left(\frac{RT}{\bar{c}} \frac{1}{\mathscr{G}'\left(\mathscr{G}^{-1}\left(\frac{c_\alpha}{\bar{c}}\right)\right)} \nabla c_\alpha + z_\alpha F \nabla \phi \right) \\ &= -D_\alpha \left(d_\alpha\left(\frac{c_\alpha}{\bar{c}}\right) \nabla c_\alpha + c_\alpha z_\alpha \frac{F}{RT} \nabla \phi \right). \end{aligned} \tag{C.7}$$

Again, it is hard to express the thermodynamical equilibrium in these variables. This fact demands additional care when devising numerical approximations. The term

$$d_\alpha\left(\frac{c_\alpha}{\bar{c}}\right) = \frac{c_\alpha}{c \mathscr{G}'\left(\mathscr{G}^{-1}\left(\frac{c_\alpha}{\bar{c}}\right)\right)} \overset{\mathscr{G}=\mathscr{F}_{-1}}{=} \frac{1}{1-\frac{c_\alpha}{\bar{c}}} \tag{C.8}$$

is the *diffusion enhancement* denoted by g_3 in [RT02, vMC08, KG12], see also [LFJ11]. This expression exhibits degenerating behaviour demanding special care during analytical and numerical treatment. Such terms also occur in “volume filling” models in chemotaxis. These have been motivated by similar considerations as in the volume exclusion models described in the present paper. In this community, the degeneration of the diffusion coefficient is termed “fast diffusion”, which may prevent overcrowding and blow-up. A significant body of work is devoted to its analysis in the concentration based setting [HP09, Wrz04, PH02, BFDS06].

Appendix D. Existence of inverse activity coefficients

D.1. **Proof of lemma 3.1.**

Proof. Denoting $b_i = a_i^\circ$, and $n = N - 1$ rewrite system (3.6) as

$$b_\alpha \beta_\alpha + \sum_{i=1}^{n} \beta_i a_i = 1 \qquad (\alpha = 1 \dots n). \tag{D.1}$$

or $M(\beta_1, \beta_2, \dots \beta_n)^T = (1, 1, \dots 1)^T$ Assume that $b_\alpha > 0, a_\alpha \geq 0$. The system matrix M can be expressed as a rank one update of an invertible diagonal matrix B:

$$M = B + u a^T \tag{D.2}$$

where $B = \mathrm{diag}(b_1, b_2, \dots b_n)$, $u = (1,1,\dots 1)^T$, $a = (a_1, a_2, \dots a_n)^T$. According to the Sherman-Morrison formula [Bar51], if $1 + a^T B^{-1} u \neq 0$, the inverse of M can be expressed as

$$M^{-1} = B^{-1} - \frac{B^{-1} u a^T B^{-1}}{1 + a^T B^{-1} u} \tag{D.3}$$

As $B^{-1} = \mathrm{diag}(b_1^{-1}, b_2^{-1}, \dots b_n^{-1})$, one gets

$$1 + a^T B^{-1} u = 1 + \sum_{i=1}^{n} a_i b_i^{-1} \tag{D.4}$$

$$u a^T = \begin{pmatrix} a_1 & a_2 & \dots & a_n \\ a_1 & a_2 & \dots & a_n \\ \vdots & \vdots & & \vdots \\ a_1 & a_2 & \dots & a_n \end{pmatrix}, \tag{D.5}$$

$$B^{-1} u a^T = \begin{pmatrix} b_1^{-1} a_1 & b_1^{-1} a_2 & \dots & b_1^{-1} a_n \\ b_2^{-1} a_1 & b_2^{-1} a_2 & \dots & b_2^{-1} a_n \\ \vdots & \vdots & & \vdots \\ b_n^{-1} a_1 & b_n^{-1} a_2 & \dots & b_n^{-1} a_n \end{pmatrix}, \tag{D.6}$$

$$B^{-1} u a^T B^{-1} = \begin{pmatrix} b_1^{-1} a_1 b_1^{-1} & b_1^{-1} a_2 b_2^{-1} & \dots & b_1^{-1} a_n b_n^{-1} \\ b_2^{-1} a_1 b_1^{-1} & b_2^{-1} a_2 b_2^{-1} & \dots & b_2^{-1} a_n b_n^{-1} \\ \vdots & \vdots & & \vdots \\ b_n^{-1} a_1 b_1^{-1} & b_n^{-1} a_2 b_2^{-1} & \dots & b_n^{-1} a_n b_n^{-1} \end{pmatrix}, \tag{D.7}$$

$$B^{-1} u a^T B^{-1} \begin{pmatrix} 1 \\ 1 \\ \vdots \\ 1 \end{pmatrix} = \begin{pmatrix} b_1^{-1} \sum_{i=1}^{n} a_i b_i^{-1} \\ b_2^{-1} \sum_{i=1}^{n} a_i b_i^{-1} \\ \vdots \\ b_n^{-1} \sum_{i=1}^{n} a_i b_i^{-1} \end{pmatrix}, \tag{D.8}$$

$$B^{-1}(1 + a^T B^{-1} u) \begin{pmatrix} 1 \\ 1 \\ \vdots \\ 1 \end{pmatrix} = \begin{pmatrix} b_1^{-1} + b_1^{-1} \sum_{i=1}^{n} a_i b_i^{-1} \\ b_2^{-1} + b_2^{-1} \sum_{i=1}^{n} a_i b_i^{-1} \\ \vdots \\ b_n^{-1} + b_n^{-1} \sum_{i=1}^{n} a_i b_i^{-1} \end{pmatrix}, \tag{D.9}$$

$$\tag{D.10}$$

As a consequence,

$$\beta_\alpha = \frac{b_\alpha^{-1}}{1 + \sum_{i=1}^{n} a_i b_i^{-1}} = \frac{1}{b_\alpha + \sum_{i=1}^{n} a_i \frac{b_\alpha}{b_i}}. \tag{D.11}$$

□

D.2. **Proof of lemma 3.2.**

Proof. Denoting $b_i = a_i^\circ \exp\left(\frac{p-p^\circ}{cRT}\right)^{1-\frac{M_\alpha}{M_N}}$, $m_\alpha = -\frac{M_\alpha}{M_N}$ and $n = N - 1$ rewrite system (3.9) as

$$(b_\alpha \beta_\alpha)^{m_\alpha} + \sum_{i=1}^{n} \beta_i a_i = 1 \qquad (\alpha = 1 \dots n). \tag{D.12}$$

The solution $\beta = (\beta_\alpha)_{\alpha=1\dots n}$ is a fixed point of the continuous mapping

$$\beta \mapsto \beta' \tag{D.13}$$

$$Q := [0, b_1^{-1}] \times [0, b_2^{-1}] \times \cdots \times [0, b_n^{-1}] \to Q \tag{D.14}$$

$$\text{defined by} \quad b_\alpha^{m_\alpha} \beta_\alpha^{m_\alpha - 1} \beta'_\alpha + \sum_{i=1}^{n} \beta'_i a_i = 1 \qquad (\alpha = 1 \dots n). \tag{D.15}$$

Under the assumption $\beta_\alpha < \frac{1}{b_\alpha}$ and noting that $m_\alpha < 0$, according to lemma 3.1, system (D.15) has a unique bounded solution

$$0 < \beta'_\alpha < \frac{\beta_\alpha^{1-m_\alpha}}{b_\alpha^{m_\alpha}} < \frac{1}{b_\alpha^{m_\alpha} b_\alpha^{1-m_\alpha}} = \frac{1}{b_\alpha}, \qquad (\alpha = 1 \dots n) \tag{D.16}$$

which continuously depends on the input data of (D.15). Thus the mapping (D.15) indeed maps the compact convex bounded domain Q into itself. By Brouwer's fixed point theorem [Dei85], it has a fixed point in Q.
Concerning uniqueness, assume that there is a second fixed point B' fulfilling (D.12). Subtracting the equations from each other and applying the mean value theorem for the difference $\delta_\alpha = \beta_\alpha - \beta'_\alpha$ yields

$$\tilde{b}_\alpha \delta_\alpha + \sum_{i=1}^{n} a_i \delta_i = 0 \qquad (\alpha = 1 \dots n),$$

where $\tilde{b}_\alpha = m b_\alpha^m \tau_\alpha^{m_\alpha - 1} > 0$ for certain $\tau_\alpha \in (\beta_\alpha, \beta'_\alpha)$. According to the proof of lemma 3.1 (replacing the right hand side by 0), this system has a unique solution which is zero. □

References

[AdP06] P. Atkins and J. de Paula. *Atkins' Physical Chemistry*. Oxford University Press, 2006.

[Bar51] M. S. Bartlett. An inverse matrix adjustment arising in discriminant analysis. *Ann. of Math. Stat.*, pages 107–111, 1951.

[BC12] M. Bessemoulin-Chatard. A finite volume scheme for convection–diffusion equations with nonlinear diffusion derived from the Scharfetter–Gummel scheme. *Numer. Math.*, 121(4):637–670, 2012.

[BF80] A. J. Bard and L. R. Faulkner. *Electrochemical methods*. Wiley New York, 1980.

[BFDS06] M. Burger, M. Di Francesco, and Y. Dolak-Struss. The Keller-Segel model for chemotaxis with prevention of overcrowding: linear vs. nonlinear diffusion. *SIAM J. Math. Anal.*, 38(4):1288–1315, 2006.

[Bik42] J. J. Bikerman. Structure and capacity of electrical double layer. *Philos. Mag.*, 33(220):384–397, 1942.

[BKSA09] M. Z. Bazant, M. S. Kilic, B. D. Storey, and A. Ajdari. Towards an understanding of induced-charge electrokinetics at large applied voltages in concentrated solutions. *Adv. Coll. Interf. Sci.*, 152(1):48–88, 2009.

[BR87] R. E. Bank and D. J. Rose. Some error estimates for the box method. *SIAM J. Numer. Anal.*, 24(4):777–787, 1987.

[BS07] P. M. Biesheuvel and M. Van Soestbergen. Counterion volume effects in mixed electrical double layers. *J. Coll. Interf. Sci.*, 316(2):490–499, 2007.

[CS69] N. F. Carnahan and K. E. Starling. Equation of state for nonattracting rigid spheres. *J. Chem. Phys.*, 51:635, 1969.

[Dei85] K. Deimling. *Nonlinear functional analysis*. Springer, 1985.

[DGL14] W. Dreyer, C. Guhlke, and M. Landstorfer. A mixture theory of electrolytes containing solvation effects. *Electrochem. Comm.*, 2014.

[dGM62] S. R. de Groot and P. O. Mazur. *Non-Equilibrium Thermodynamics*. Dover Publications, 1962.

[DGM13] W. Dreyer, C. Guhlke, and R. Müller. Overcoming the shortcomings of the Nernst-Planck model. *Phys. Chem. Chem. Phys.*, 15:7075–7086, 2013.

[EB11] M. Eikerling and P. Berg. Poroelectroelastic theory of water sorption and swelling in polymer electrolyte membranes. *Soft Matter*, 7(13):5976–5990, 2011.

[EFG06] R. Eymard, J. Fuhrmann, and K. Gärtner. A finite volume scheme for nonlinear parabolic equations derived from one-dimensional local Dirichlet problems. *Numer. Math*, 102(3):463 – 495, 2006.

[EGH00] R. Eymard, T. Gallouët, and R. Herbin. Finite volume methods. In *Handbook of numerical analysis, Vol. VII*, pages 713–1020. North-Holland, 2000.

[Fre52] V. Freise. Zur Theorie der diffusen Doppelschicht. *Z. Elektrochem*, 56:822–827, 1952.

[GG09] A. Glitzky and K. Gärtner. Energy estimates for continuous and discretized electro-reaction–diffusion systems. *Nonlinear Analysis*, 70(2):788–805, 2009.

[HP09] T. Hillen and K. J. Painter. A user's guide to PDE models for chemotaxis. *J. Math. Biol.*, 58(1-2):183–217, 2009.

[IUP14] IUPAC compendium of chemical terminology. URL: http://goldbook.iupac.org/, 2014. Accessed 2014-04-01.

[KG12] Th. Koprucki and K. Gärtner. Discretization scheme for drift-diffusion equations with a generalized Einstein relation. Technical report, Weierstrass Institute, 2012. WIAS Preprint No. 1738.

[KV81] A. A. Kornyshev and M. A. Vorotyntsev. Conductivity and space charge phenomena in solid electrolytes with one mobile charge carrier species, a review with original material. *Electrochim. Acta*, 26(3):303–323, 1981.

[LFJ11] M. Landstorfer, S. Funken, and T. Jacob. An advanced model framework for solid electrolyte intercalation batteries. *Phys. Chem. Chem. Phys.*, 13(28):12817–12825, 2011.

[LL86] L. D. Landau and E. M. Lifshitz. *Hydrodynamics [in Russian]*. Nauka, Moscow, 1986.

[Mac53] R. H. Macneal. An asymmetrical finite difference network. *Quart. Math. Appl.*, 11:295–310, 1953.

[MCSJ71] G. A. Mansoori, N. F. Carnahan, K. E. Starling, and T. W. Leland Jr. Equilibrium thermodynamic properties of the mixture of hard spheres. *J. Chem. Phys.*, 54:1523, 1971.

[MR02] M. Manciu and E. Ruckenstein. Lattice site exclusion effect on the double layer interaction. *Langmuir*, 18(13):5178–5185, 2002.

[Mü85] I. Müller. *Thermodynamics*. Interaction of Mechanics and Mathematics. Pitman, 1985.

[NTA12] J. Newman and K. E. Thomas-Alyea. *Electrochemical systems*. Wiley-Interscience, 2012.

[PDK+96] V. N. Paunov, R. I. Dimova, P. A. Kralchevsky, G. Broze, and A. Mehreteab. The hydration repulsion between charged surfaces as an interplay of volume exclusion and dielectric saturation effects. *J. Colloid Interf. Sci*, 182(1):239–248, 1996.

[PH02] K. J. Painter and T. Hillen. Volume-filling and quorum-sensing in models for chemosensitive movement. *Can. Appl. Math. Quart*, 10(4):501–543, 2002.

[Rou06] T. Roubíček. Incompressible ionized fluid mixtures. *Cont. Mech. Thermodyn.*, 17(7):493–509, 2006.

[RT02] Y. Roichman and N. Tessler. Generalized Einstein relation for disordered semiconductors—implications for device performance. *Appl. Phys. Lett.*, 80(11):1948–1950, 2002.

[SF+14] T. Streckenbach, J. Fuhrmann, et al. Pdelib- a software toolbox for numerical computations. URL: http://www.pdelib.org, 2014. Accessed 2014-01-15.

[SG69] D. L. Scharfetter and H. K. Gummel. Large signal analysis of a silicon Read diode. *IEEE Trans. Electron. Dev.*, 16:64–77, 1969.

[SGF10] H. Si, K. Gärtner, and J. Fuhrmann. Boundary conforming Delaunay mesh generation. *Comput. Math. Math. Phys.*, 50:38–53, 2010.

[SGK+14] O. Schenk, K. Gärtner, G. Karypis, S. Röllin, and M. Hagemann. PARDISO Solver Project. URL: http://www.pardiso-project.org, 2014. Accessed 2014-01-15.

[She] J. Shewchuk. Triangle: A two-dimensional quality mesh generator and Delaunay triangulator. URL: http://www.cs.cmu.edu/ quake/triangle.html. Accessed 2014-04-01.

[Si14] H. Si. TetGen version 1.5. URL: http://tetgen.org/, 2014. Accessed 2014-04-01.

[Spa58] M. J. Sparnaay. Corrections of the theory of the flat diffuse double layer. *Recueil des Travaux Chimiques des Pays-Bas*, 77(9):872–888, 1958.

[Ste24] O. Stern. Zur Theorie der elektrolytischen Doppelschicht. *Z. f. Electrochemie*, 30:508, 1924.

[Tre08] G. Tresset. Generalized Poisson-Fermi formalism for investigating size correlation effects with multiple ions. *Phys. Rev. E*, 78(6):061506, 2008.

[vMC08] S. L. M. van Mensfoort and R. Coehoorn. Effect of Gaussian disorder on the voltage dependence of the current density in sandwich-type devices based on organic semiconductors. *Phys. Rev. B*, 78(8):085207, 2008.

[Wrz04] D. Wrzosek. Global attractor for a chemotaxis model with prevention of overcrowding. *Nonlinear Anal.*, 59(8):1293–1310, 2004.